



Highly porous spark plasma sintered Ni-Mn-Ga structures



Frans Nilsén*, Joonas Lehtonen, Yanling Ge, Ilkka Aaltio, Simo-Pekka Hannula

Aalto University, Espoo 00076, Finland

ARTICLE INFO

Article history:

Received 5 May 2017

Received in revised form 22 June 2017

Accepted 22 June 2017

Available online xxx

Keywords:

Spark plasma sintering

Ferromagnetic shape memory alloy

Porous material

Magnetic-field-induced strain

ABSTRACT

A new approach for the processing of porous crystalline Ni-Mn-Ga compacts by spark plasma sintering (SPS) from a mixture of gas atomized Ni-Mn-Ga and NaCl powders (25/75 vol%) is reported. The NaCl was removed to reveal a highly porous skeleton of Ni-Mn-Ga. Solid skeletons were heat-treated in vacuum to grow the grains to a size of 22–23 μm , from the 1.7 μm found in the powder. The sample with the highest porosity showed a magnetic-field-induced strain of 1.24%. The MFIS is attributed to magnetically induced twinning due to the reduction of grain boundary constraints and the formation of preferred orientation.

© 2016 Acta Materialia Inc. Published by Elsevier Ltd. All rights reserved.

Ni-Mn-Ga alloys have attracted attention as magnetic shape memory material due to giant magnetic-field-induced strains (MFIS) that makes them suitable for actuators [1]. Previously large MFIS has been found only in single crystal structures [1]. The low MFIS of polycrystalline Ni-Mn-Ga has been ascribed to grain boundary constraints, which hinder twin movements in the deforming grains by creating incompatible stresses between them [2]. Two ways have been used to increase the MFIS of polycrystalline Ni-Mn-Ga, i.e., by increasing the porosity [2], which reduces the constraints, and by introducing a texture for example by directional solidification that creates preferred grain orientation [3]. Such coarse-grained Ni-Mn-Ga foams that have been manufactured using special casting replication technique concomitant with directional solidification have reached MFIS of 0.65% [3]. In the present study, we propose a new, simple, and fast approach for producing high porosity Ni-Mn-Ga structures i.e. spark plasma sintering (SPS) of a composite of MSM powder and spaceholder powder.

Spark plasma sintering (i.e. pulsed electric current sintering) is a fast sintering method, which uses pulsed direct electric current and uniaxial compressive stress to consolidate powders. In comparison to other sintering techniques, in SPS the heating power is not distributed evenly over the volume of the powder but is instead focused on the contact regions where the powder particles are touching [4]. This leads to fast and efficient sintering with accurate control over the sintering process. The main advantage of SPS is that instead of multiple processing steps as e.g. in casting replication method, porous structures can be manufactured by sintering a powder mixture with Ni-Mn-Ga powder and a suitable spaceholder material such as NaCl [5] in one single step.

Gas atomized Ni-Mn-Ga powder was used in SPS. The starting composition for the gas atomized powder was $\text{Ni}_{49.4}\text{Mn}_{28.9}\text{Ga}_{21.7}$. Atomization was carried out at 1308 °C using argon gas atomization at a pressure of 50 bars. In comparison to crushed powder produced e.g. by mechanical milling, gas atomization results in dense spherical particles with smooth surfaces, a narrow particle size distribution and lower sintering temperature [4,6]. The regular shape and smooth surfaces of the powder leads to higher packing density, which in turn lowers the sintering temperature [4]. In the present study, five different Ni-Mn-Ga foams are manufactured from a mixture of gas atomized Ni-Mn-Ga powder and NaCl powder using SPS. The effect of SPS parameters on the porosity, chemical composition, magnetization, texture and the magnetic-field-induced strain are studied after the removal of the NaCl spaceholder.

A powder mixture consisting 25 vol% of gas atomized $\text{Ni}_{49.7}\text{Mn}_{28.4}\text{Ga}_{21.9}$ powder with mean particle size of 15.2 μm and 75 vol% of coarse NaCl powder (Ensure® sodium chloride from VWR) with mean particle size of 330 μm , was prepared by mixing the two components in a Willy Bachofen Turbula shaker-mixer at room temperature for 2 h. For the processing of the five SPS samples (named here after SPS 1, SPS 2, SPS 3, SPS 4 and SPS 5) 13 g of the powder mixture was placed in 20 mm diameter graphite mold with a protective graphite foil between mold and powder. The sample was compressed at room temperature using a pressure, which was varied from 0 to 50 MPa depending on the sample. The sample was then spark plasma sintered using FCT HP D 25-2 pulsed electric current sintering unit. The sintering temperature was kept at 700 °C i.e., below the melting point of NaCl (800.7 °C [7]). During consolidation, the pulse length was 10 ms and the pause between pulses 5 ms. During heating and cooling the rates were kept constant. Sintering time and pressure as well as the room-

* Corresponding author.

E-mail address: frans.nilsen@aalto.fi (F. Nilsén).

Table 1

Sintering parameters that were varied during the sintering, grain size after sintering (SPS) and after heat-treatment (HT) and porosities after heat-treatment.

	Sintering time [min]	Sintering pressure [MPa]	Pre-compression [MPa]
SPS 1	45	25	50
SPS 2	30	25	50
SPS 3	15	50	0
SPS 4	15	25	50
SPS 5	45	50	0

	Grain size after SPS [μm]	Grain size after HT [μm]	Porosity [%]
SPS 1	10.4 ± 0.6	24.2 ± 1.6	81.0 ± 0.9
SPS 2	12.1 ± 0.6	24.6 ± 1.6	63.1 ± 1.8
SPS 3	10.4 ± 0.6	24.3 ± 1.6	80.6 ± 1.8
SPS 4	11.2 ± 0.6	22.9 ± 1.6	86.9 ± 1.8
SPS 5	10.5 ± 0.6	24.8 ± 1.6	92.3 ± 1.8

temperature pre-compression pressure were varied for the samples (Table 1).

After sintering, the protective foil was grinded off. The salt was dissolved immersing the sample into 1 l of deionized water for 48 h. Water was changed every 12 h and throughout the dissolution a magnetic stirrer was used to circulate the water within the sample, which was placed on a net basket in the middle of the beaker. After removal of the salt, the samples were heat-treated in evacuated quartz ampoules. Sample SPS 1 was kept at 900 °C for 24 h while other samples were kept at 1000 °C for 48 h. In sample SPS 1 the powder particles detached easily and the resulting foam structure was not rigid and was easily broken. The longer heat-treatment time and higher temperature used in processing of the other samples led to the formation of a firm porous structure, where the original boundaries between the particles could no longer be seen. Specimens for further studies were cut from the SPS pieces. The samples were rectangular cuboids, with dimensions z ($3.70 \text{ mm} \pm 0.89 \text{ mm}$) parallel to the direction stress and directions x ($4.19 \text{ mm} \pm 0.85 \text{ mm}$) and y ($10.51 \text{ mm} \pm 1.73 \text{ mm}$) perpendicular to the direction of stress (see Supplementary material).

Porosities were measured by AccuPyc™ 1330 pycnometer using the helium gas displacement method to measure the relative density of each sample. The porosity was then calculated using the theoretical density of 7.91 g/cm^3 [6]. The highest porosity 92% was found in sample SPS 5 (Table 1), which was sintered for 45 min at the pressure of 50 MPa without any pre-compression, while the lowest was 63% in SPS 2. Even though the mixing time and the nominal ratio of Ni-Mn-Ga and NaCl powders in the mixture were the same for each sample, differences in the porosity can be formed during the mold filling stage due to segregation of powders having different sizes and densities. After the salt removal, it could be observed that the upper part of each SPS sample had larger porosity in the top part indicating that segregation of heavier and smaller MSM powder had occurred during the filling of the mold. During sample cutting it was noted that larger pores and larger porosity existed in the surface layer of the SPS samples. However, as the specimens for further studies were cut from inside the SPS samples, there was no porosity gradient in the specimens. Thus, the changing porosity in the surface of the SPS samples had no effect on the studied properties such as MFIS, VSM and XRD texture. The increased porosity can be seen in the edges of the optical microscope images that were taken at $2.5\times$ magnification (Fig. 1a and Supplementary material). This effect, which results from the segregation of salt during the packing of the powder sample depends on the size distribution of NaCl powder.

The grain size of the atomized powder and the sintered samples before and after heat-treatment, was studied using optical microscope (Leica DRMx). Samples were cast in Epofix-epoxy and etched using a solution of 20 ml HCl, 20 ml HNO_3 , 8 ml H_3PO_4 and 40 ml of CH_3COOH (Fig. 1b). The grain size of the gas atomized Ni-Mn-Ga powder was $1.7 \pm 0.2 \mu\text{m}$. During the sintering process, the grain size increased six-

fold (up to 10–12 μm) and the following heat-treatment further doubled the grain size to about 22–24 μm (Table 1). As the DV50 of the powder was 15 μm (with a mode of 16 μm and a span of 2.05), the grain size has grown larger than the original particle size. Chemical composition of the gas atomized powder and the samples was determined using Thermo NSS EDX attached to Tescan Mira 3 SEM and with Oxford INCA EDX attached to LEO 1450 SEM using a known reference. The compositional analysis based on the EDX results (Table 2) show that manganese evaporation during the process is small. The phase transformation temperatures were measured using a low-field *ac* magnetic susceptibility measuring system in the temperature range of $-60 \text{ }^\circ\text{C}$ to $120 \text{ }^\circ\text{C}$. The values presented in Table 2 are average values of the start and finish temperatures of the phase transformation. The martensite transformation temperature (T_m) of the gas atomized powder was at $35.1 \text{ }^\circ\text{C}$ and the austenite transformation (T_a) at $42.1 \text{ }^\circ\text{C}$. As such, the SPS treatment in combination with the heat treatment has led to slightly elevated phase transformation temperatures (Table 2).

The effect of increased structural ordering and homogeneity, as well as the relief of internal stresses during annealing has resulted in the increase in phase transformation temperatures. This is evidenced by the small hysteresis in the magnetic susceptibility curve at the phase

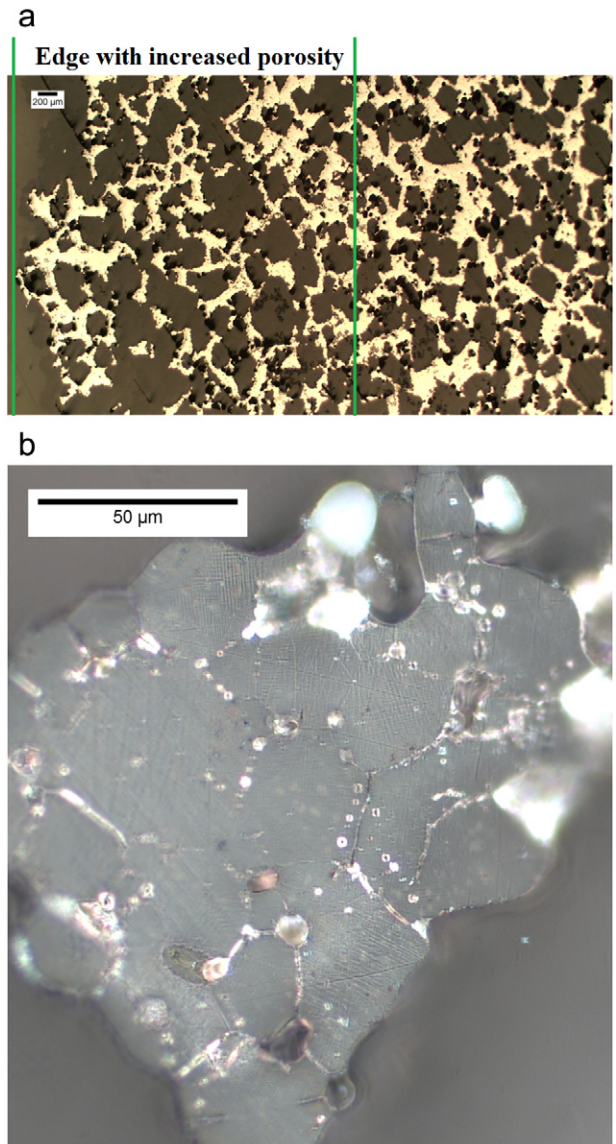


Fig. 1. Optical microscope images of sample SPS 5 zy-plane with (a) $2.5\times$ magnification without etching and (b) with $50\times$ magnification with etching and polarization.

Download English Version:

<https://daneshyari.com/en/article/5443444>

Download Persian Version:

<https://daneshyari.com/article/5443444>

[Daneshyari.com](https://daneshyari.com)